Analysis of Concrete Arch Shells for Agricultural and Light Industrial Buildings

by
Robert L. Mensch
and G. L. Nelson

Technical Bulletin, No. T-107
February 1964

CONTENT

Analysis of Concrete Arch Shells For Agricultural and Light Industrial Buildings

by

Robert L. Mensch and G. L. Nelson
Department of Agricultural Engineering

Pneumatic placement of concrete on semi-circular or parabolic shaped forms is a new concept in reinforced concrete construction. This produces a concrete arch shell building with the well-accepted "Quonset" shape and the durability of concrete (Figure 1).

This bulletin reports results of a study to evaluate and compare theoretical and actual behavior of concrete arch shells.

Experiments (4) with model arches, load-tested in the laboratory, were conducted at the Oklahoma Station to investigate the structural

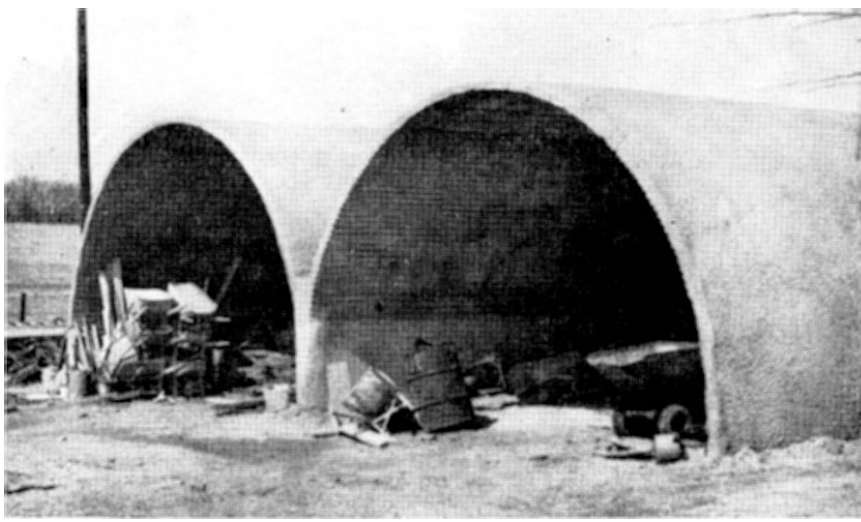

Figure 1. Circular concrete shell arch utility building.

Acknowledgement
Grateful acknowledgement is given to the Portland Cement Association, Chicago, Illinois, for their financial support of this investigation.
Research reported herein was done under Station Project 633.

behavior of concrete arch shells of circular and parabolic shapes. Analytical studies were made to develop analysis and design parameters for various loading arrangements on arches of any size and of circular and parabolic configurations.

Objectives

A theoretical study was conducted to develop generalized analytical methods for quick computation of transverse shear, bending moment and direct stress throughout an arch and deflection of its peak: (1) for any size arch; (2) of circular or parabolic shape; (3) with fixed or hinged end conditions; (4) for each type of load distribution usually considered in the design of light structures.

The purpose of the experimental investigation was to determine:

1. Added arch stiffness achieved by fixed compared to hinged supports.
2. Ultimate load carrying capacity.
3. Effects of repetitive loading.
4. Effects from each phase of each load-unload cycle.

Assumptions

Assumptions in planning this investigation were:

1. Results from model arches would be representative of prototype structures.
2. Circular arches were best for experimental work since their theoretical stresses are higher under most loads than stresses in parabolic arches.
3. Basic principles of reinforced concrete are applicable to thin concrete sections.

Experimental Investigation

Eight circular model arches were built and tested. Each arch had a span of 10 feet, width of 1 foot and thickness of 2 inches with 4″ x 4″-4/4 welded wire fabric placed at mid-depth. Ultimate bending moment computed from these cross-section dimensions and a concrete fibre stress of 4500 psi was 7350 in-lbs; for a stress in the steel of 40,000 psi the ultimate bending moment was 4650 in-lbs.

The model arches were built by a contractor who specialized in pneumatic placement of concrete. Figure 2 shows this method being used for casting another set of experimental arches. The model arches in the present study were cast indoors in the laboratory. The major items of equipment were a special mixing machine and a high capacity air compressor. The mixing machine mixed the ingredients to a controlled water-cement ratio, then forced the mixture by compressed air through a large diameter hose terminating in a special nozzle from which the concrete was shot to the point of application. With this type of equipment, more sand and less coarse aggregate are usually used. Coarse aggregate as large as $\frac{3}{8}$ to $\frac{1}{2}$ in. in size may be used. It is possible to mix and place concrete having a smaller slump and higher strength than obtained with usual water-cement ratios.

A total of eight model arches were load-tested in the laboratory; four with fixed end conditions and four with hinged ends. Figure 3 illustrates one arch installed for test. Strain gages were located as close

Figure 2. Pneumatic placement of wet-mix concrete for casting experimental shell arches.

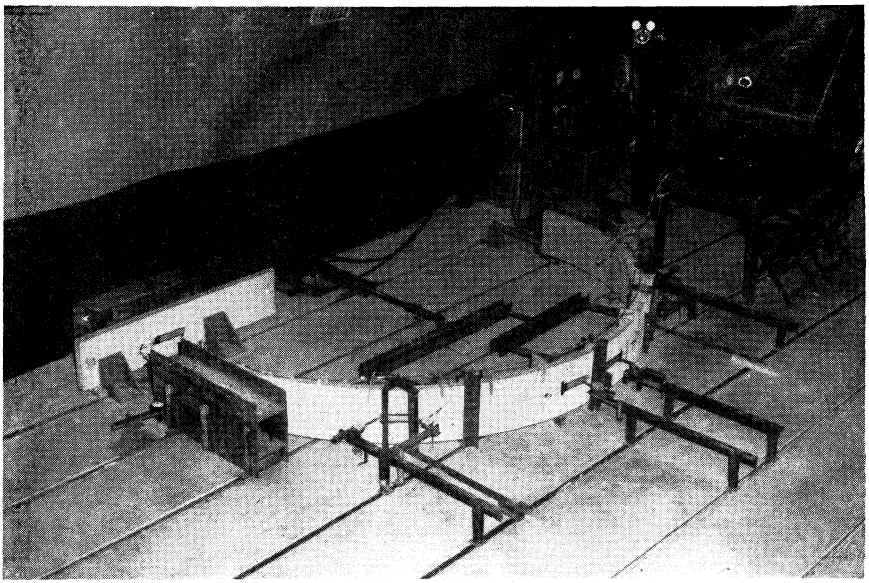

Figure 3. Model concrete shell arches installed for laboratory load-testing experiments.

as possible to the points of maximum theoretical moment. Three equal point loads were applied as shown in Figure 4. Strain and deflection were measured at critical points during three load-unload cycles. Finally, each arch was subjected to an ultimate load test in which the load was increased until the arch collapsed.

No significant differences in the load-deflection characteristics occurred between the fixed and hinged end arches, as revealed by the ultimate load tests. The load-deflection characteristics are shown in Figures 5 and 6. The average ultimate load was 765 lbs per load point or a total of 2295 lbs. The maximum load predicted by elastic theory was 530 lbs per load point on the fixed end arches, and 615 lbs on the hinged end arches. In the fixed end arches, the largest moment theoretically occurred at the supports. It is hypothesized that, during testing, plastic hinges developed at the supports. The formation of plastic hinges caused a redistribution of stresses and increased the load carrying capacity of the arch.

To accurately compare the measured strain and deflection with theoretical predictions, it was necessary to determine the stiffness modulus, EI, of the concrete cross section used in the arches. For this determi-

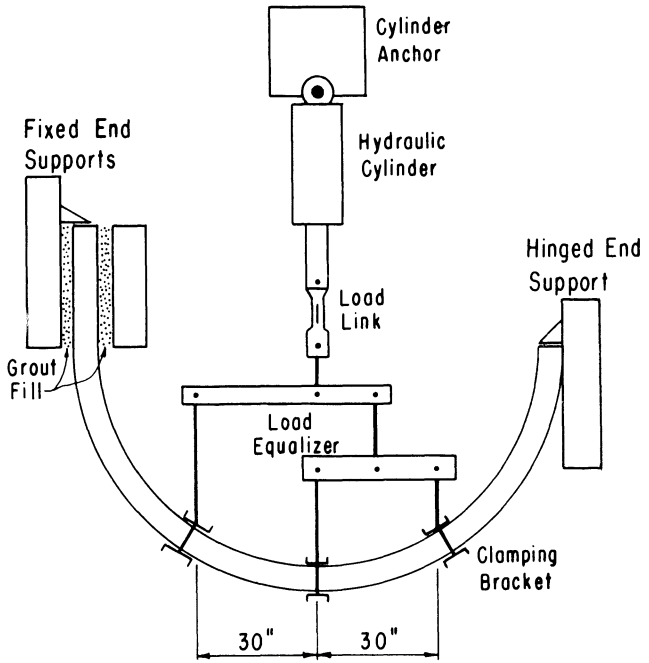

Figure 4. Load and support brackets for laboratory load-testing of model concrete shell arches.

nation, straight slabs which had the same cross section and reinforcement and were cast by the same method as the arches were tested as simple beams. A tabulation of EI values for the slabs and arches is given in Table I. Of all the EI's computed, the lowest and safest one for design purposes was the one based on the usual assumption of reinforced concrete design that concrete does not resist tensile stresses.

Theoretical Investigation

In this investigation, the effects were analyzed of several loading conditions and two end restraint conditions on circular and parabolic arches. The outline of the arches is shown in Figure 7. In the parabolic arch the ratio of R/S was 0.625; which appeared to be desirable for appearance and utility of space within the structure.

In a statically indeterminate arch, the reactions and moments at one location are first evaluated by an elastic analysis. Then the analysis can be completed by statics. The area-moment formulas derived from elastic analysis were used to determine the reactions and moment at one support.

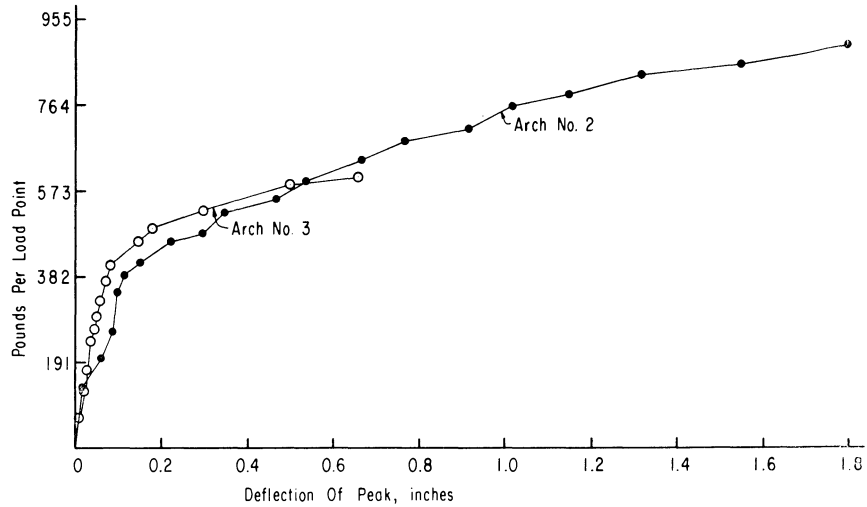

Figure 5. Load-deflection curves for fixed end arches.

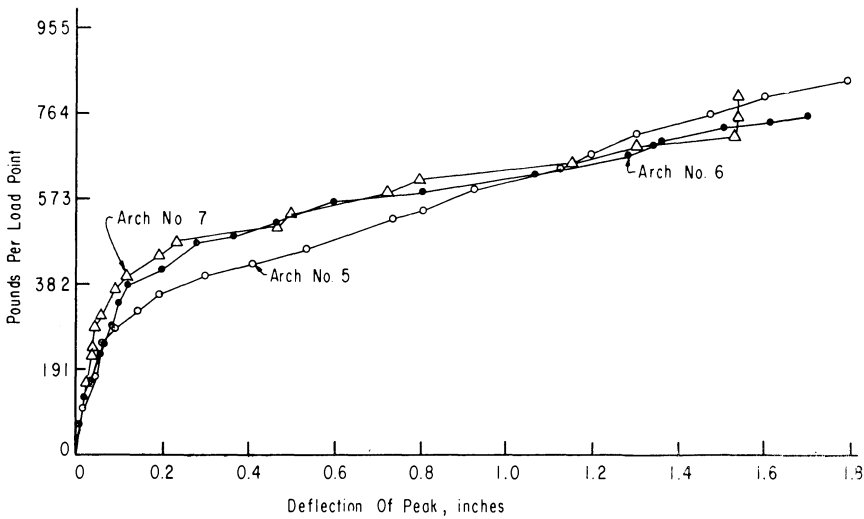

Figure 6. Load-deflection curves for hinged end arches.

In the fixed end arches, the movement of the supports was assumed to be zero. For the hinged end arches; free rotation of the ends without displacement was assumed. The arches had a constant stiffness modulus, EI, throughout. Therefore, it was not necessary to specify a value for EI to analyze the arch.

TABLE I—Comparison of Methods Used to Determine Stiffness Modulus.

Method of Computation	EI Value $\times 10^{-6}$	Remarks
Analytical:		
When concrete does NOT resist tension.	2.25	This is safest value computed. This theory commonly used in reinforced concrete design work.
When concrete does resist tension.	36.0	Computed with neutral axis at centroid of cross section. E_c equal to 4.5×10^6 and I equal to 8 in^4.
Experimental:		
Deflection of slabs	3.518	These 3 slabs had shrinkage cracks about every 4 inches.
	12.082	Two of these three slabs had no visible cracks before testing. Some concrete is apparently resisting tension.
Strain in slabs	31.621	Applied moment determined from the loading arrangement. Strain diagrams showed neutral axis at centroid of section.
Deflection of arches;		
fixed end	15.392	Differences in observed deflection between fixed and hinged end conditions was small. Differences in computed $EI\Delta Y_p$ caused the large differences in EI.
hinged end	31.588	
Strain in arches;		
top of fixed end arch	30.028	Large values indicate actual moment was not as great as computed theoretically. Theoretical moments used to compute these values of EI.
base of fixed end arch	85.768	
top of hinged end arch	61.308	
45° point hinged end	25.714	

Design Loads and Load Distribution Equations

Each applied load was described in mathematical terms so that shears and moments could be computed by area-moment analysis. Load distribution equations were written for the X and Y components of each load. W_x and W_y in subsequent notations are the load intensities in the X and Y directions respectively. The units of these quantities are lb/ft, where the length dimension, feet, is measured along the Y and X axes respectively.

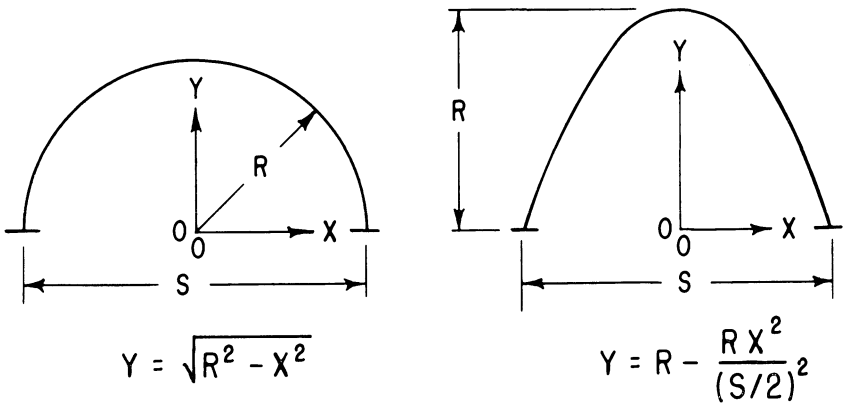

Figure 7. Equations for arch outline configurations.

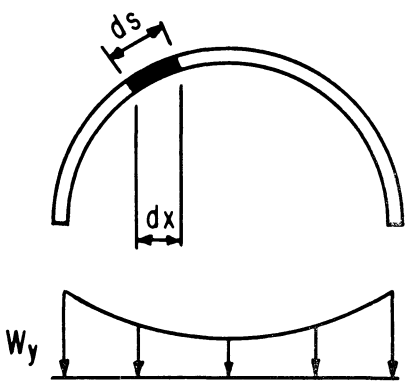

Dead Load—the dead load, DL, is the weight of one square foot of roof surface. For a concrete roof with a density of 150 lb/ft^3, DL is equal to 12.5 lb/ft^2 for each inch of roof thickness.

DL = lb/ft^2 of roof surface

$W_y = (-DL)\ (dS/dX)$ x 1 ft.

Figure 8 illustrates the nomenclature for evaluating dead load.

Figure 8. Dead load generalized diagram.

Snow Load—Design snow loads used were those recommended by the Housing and Home Finance Agency (3). A minimum value of 10 psf should be used for sleet and ice loading which may accompany snow loading. These values are in pounds per square foot of horizontal projection of roof area.

Roof Slope	3/12	6/12	9/12	12/12
Southern States	20	15	12	10
Central States	25	20	15	10
Northern States	30	25	15	10
Great Lakes, New England and mountain areas	40	30	20	10

A snow load distribution equation was developed from these recommended values. Figure 9 shows the distribution curve for each of the four geographical areas and the corresponding value of SL which is used in further calculations.

$$SL = \text{lb/ft}^2 \text{ of horizontal projected roof area}$$
$$W_y = (-SL) \;/\; (|dY/dX| + 1) \times 1 \text{ ft.}$$

Wind Load—Barre and Sammet (1) recommended a basic design load of 20 lb/ft^2 in Oklahoma for wind on a vertical plane surface. This is the stagnation pressure produced by a wind speed of 87 mph and standard air density. Building shape and wall openings modify the pressure on the building surface according to dimensionless pressure coefficients. These coefficients as given in ref. (2) for circular and parabolic arch roofs are illustrated in Figure 10.

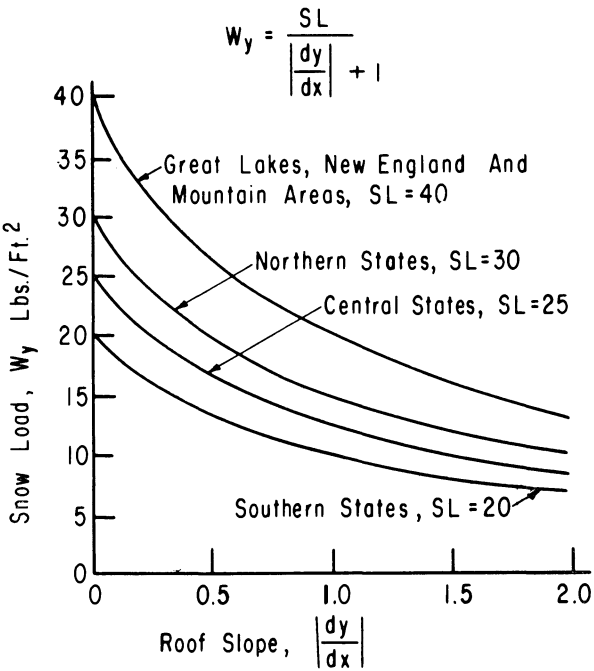

Figure 9. Snow load distribution curves.

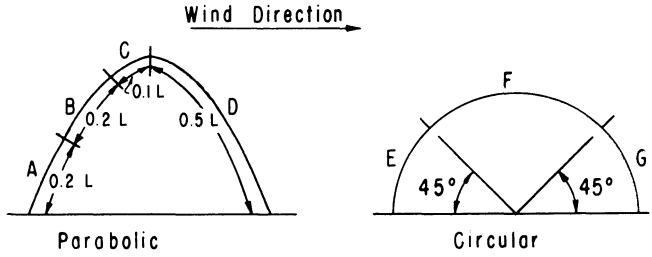

A	B	C	D		E	F	G
+1.0	+0.6	-0.35	-1.04	Closed Building	+0.613	+0.7	-0.58
+0.4	0	+0.95	-1.64	Opening On Windward Side	+0.013	-1.3	-1.18
+1.4	+1.0	+0.05	-0.64	Opening On Leeward Side	+1.013	-0.3	-0.18

Figure 10. Wind pressure coefficients.

WL = lb/ft^2 stagnation pressure on vertical surface
PC = Wind pressure normal to roof surface $\div$ stagnation wind pressure
W_y = (−PC) (WL) $\times$ 1 ft.
W_x = (PC) (WL) $\times$ 1 ft.; + when X < 0, — when X > 0

Grain Load—There are wide variations in grain storage pressures due to variations in bin configuration and characteristics of the grain. Grain pressures in vertical-walled bins may be found by use of Rankine's formula. The walls are not vertical in circular or parabolic arches and Rankine's formula is inappropriate. In the present analysis, the following equivalent fluid densities of grain are applicable:

Equivalent Fluid Densities of Common Grains, lb/ft^3

Barley	15.6
Corn, Shelled	18.0
Wheat	18.3 to 21.5

GL = lb/ft^3 equivalent fluid density of grain
YG−Y = Depth below grain level
W_x = (GL) (YG−Y) $\times$ 1 ft.; + when X > 0, − when X < 0

Figure 11 illustrates the nomenclature for grain load analysis.

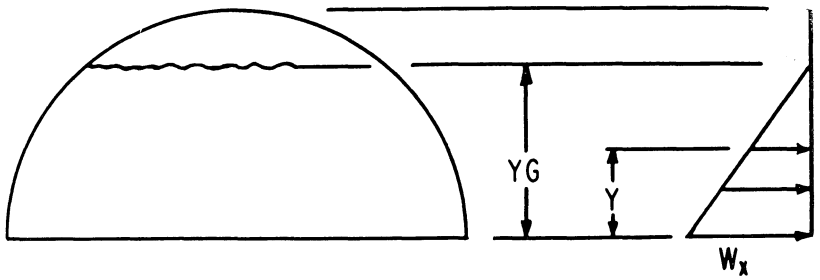

Figure 11. Grain load generalized diagram.

Concentrated Load—Arch shell buildings may carry concentrated or point loads such as an overhead crane rail or materials handling equipment suspended from the roof. In this study, the effect of point loads applied at the arch peak were analyzed.

CL = lb/ft at peak along long axis of building.

Dimensionless Design and Analysis Parameters

With the aid of dimensional analysis, dimensionless parameters were developed. These can be used to compute shear, moment and deflection for any arch geometrically similar to the ones considered in the present study.

Table II shows the pertinent quantities that describe the structural properties of an arch and the loads which may be applied to it. The values of M, V, SL, WL, GL, DL, CL, and EI are based on an arch width of one foot regardless of span. Therefore, the units are in a different form than usually associated with the quantities. The usual units have been multiplied by 1 foot to obtain the units in Table II. For example, the units of snow load, SL, were originally lb/ft^2 but are shown as lb/ft of span for an arch 1 ft wide.

The subscripts for M and V indicate location on the arch. The subscripts "i" have a numerical value for each location. The value is:

$$i = X/S$$

where "X" is horizontal distance from midspan and "S" is span.

According to the Buckingham Pi theorem, a system involving Q quantities and N basic dimensions requires (Q−N) dimensionless parameters to mathematically describe the system. The parameters are defined in Table III.

TABLE II—Pertinent Quantities.

Moment	Shear	Deflection	Variable	Units	Dimensions
M_i			Moment	ft-lb	FL
	V_i		Shear	lb	F
		D	Deflection at peak	ft	L
S	S	S	Span	ft	L
SL	SL	SL	Snow Load	lb/ft	FL^{-1}
WL	WL	WL	Wind Load	lb/ft	FL^{-1}
GL	GL	GL	Grain Load	lb/ft^2	FL^{-2}
DL	DL	DL	Dead Load	lb/ft	FL^{-1}
CL	CL	CL	Concentrated load	lb	F
		EI	Stiffness modulus	$lb\text{-}ft^2$	FL^2
7	7	8	Number of variables		
2	2	2	Number of dimensions		
5	5	6	Numbers of dimensionless terms required		

TABLE III—Parameters for Analysis of Shell Arches.

LOAD	MOMENT PARAMETER λ_i		HORIZONTAL SHEAR PARAMETER Ψ_i		VERTICAL SHEAR PARAMETER Ω_i		DEFLECTION PARAMETER δ	
	FORM	VALUE	FORM	VALUE	FORM	VALUE	FORM	VALUE
DEAD	$M_i/(DL)S^2$	Figs. 12-13	$VX_i/(DL)S$	Table IV	$VY_i/(DL)S$	Figs. 32-33	$\frac{D_p EI}{S^4(DL)}$	Table IV
SNOW	$M_i/(SL)S^2$	Figs. 14-15	$VX_i/(SL)S$	Table IV	$VY_i/(SL)S$	Figs. 34-35	$\frac{D_p EI}{S^4(SL)}$	
WIND	$M_i/(WL)S^2$	Figs. 16-19	$VX_i/(WL)S$	Figs. 24-29	$VY_i/(WL)S$	Figs. 36-41	$\frac{D_p EI}{S^4(WL)}$	
GRAIN	$M_i/(GL)S^3$	Figs. 20-21	$VX_i/(GL)S^2$	Figs. 30-31	$VY_i/(GL)S^2$	Table IV	$\frac{D_p EI}{S^5(GL)}$	
CONCEN-TRATED	$M_i/(CL)S$	Figs. 22-23	$VX_i/(CL)$	Table IV	$VY_i/(CL)$	Table IV	$\frac{D_p EI}{S^3(CL)}$	

Each of the dimensionless parameters in Table III were evaluated for two arch configurations (circular and parabolic), and two support conditions (hingeless and hinged) at 51 locations, corresponding to 51 values of "i", by a computer program. The results of the computations for the moment and shear parameters are shown in Figures 12 through 41 except for shear parameters which were constant through the arch, or only changed sign at midspan. These latter values are listed in Table IV. The value of the deflection coefficients, δ, for the arch peak are listed in Table V. Table III provides a cross-reference to the figure or table in which each parameter is evaluated.

TABLE IV—Shear Parameters for Analysis of Shell Arches.

Load	Arch Configuration	Horizontal Shear Parameters Ψ_i				Vertical Shear Parameters Ω_{-i}			
		Hingeless		2-Hinged		Hingeless		2-Hinged	
		Left Half	Right Half	Left Half	Right Half	Left Half	Right Half	Left Half	Right Half
Dead	Circular	−0.319	−0.319	−0.252	−0.252	Fig. 32	Fig. 32	Fig. 32	Fig. 32
	Parabolic	−0.271	−0.271	−0.289	−0.289	Fig. 33	Fig. 33	Fig. 33	Fig. 33
Snow	Circular	−0.206	−0.206	−0.153	−0.153	Fig. 34	Fig. 34	Fig. 34	Fig. 34
	Parabolic	−0.121	−0.121	−0.115	−0.115	Fig. 35	Fig. 35	Fig. 35	Fig. 35
Grain	Circular	Fig. 30	Fig. 30	Fig. 30	Fig. 30	−0.001	−0.001	−0.001	−0.001
	Parabolic	Fig. 31	Fig. 31	Fig. 31	Fig. 31	0.000	0.000	−0.001	−0.001
Concentrated	Circular	−0.459	−0.459	−0.320	−0.320	+0.500	−0.500	+0.500	−0.500
	Parabolic	−0.353	−0.353	−0.302	−0.302	+0.500	−0.500	+0.500	−0.500

TABLE V—Deflection Parameters for Analysis of Shell Arches.

	VALUES OF δ			
	CIRCULAR ARCH		PARABOLIC ARCH	
LOAD	FIXED	HINGED	FIXED	HINGED
DEAD	-3.93×10^{-4}	-8.29×10^{-4}	$+8.32 \times 10^{-5}$	$+1.59 \times 10^{-4}$
CONCENTRATED	-1.46×10^{-3}	-2.36×10^{-3}	-4.61×10^{-4}	-6.73×10^{-4}
GRAIN	-9.34×10^{-5}	-2.15×10^{-4}	-1.04×10^{-4}	-2.27×10^{-4}
SNOW	-3.86×10^{-4}	-7.27×10^{-4}	-3.88×10^{-5}	-6.15×10^{-5}
WIND, BLDG CLOSED	$+2.90 \times 10^{-4}$	$+5.37 \times 10^{-4}$	-5.02×10^{-6}	-8.61×10^{-6}
WIND, OPEN LEEWARD	$+2.91 \times 10^{-4}$	$+5.40 \times 10^{-4}$	$+1.47 \times 10^{-4}$	$+2.83 \times 10^{-4}$
WIND, OPEN WINDWARD	$+2.90 \times 10^{-4}$	$+5.32 \times 10^{-4}$	-2.33×10^{-4}	-4.46×10^{-4}

The value of each parameter for a specified kind of load is constant for each indexed location on the arch for all arches geometrically similar in outline and 1 ft wide, with the same end support conditions. This statement is based on the requirement that the stiffness modulus, EI, of the arch analyzed is uniform throughout the span. These parameters can be used to analyze the effect of changes in span, load intensity or stiffness modulus on moment, shear, and direct stresses. Figure 42 shows the sign convention assumed for shears and moment.

In most design work, the span, load and stiffness modulus are known or assumed, from which the designer must calculate the shear, direct stresses and moments which result. Analytical equations can be obtained from the parameters to compute moment, horizontal and vertical shearing forces and deflections as follows:

$$M_i = \lambda_i \; (\_L \; S^p) \qquad \text{Eq. 1}$$

$$VX_i = \Psi i \; (\_L \; S^q) \qquad \text{Eq. 2}$$

$$VY_i = \Omega i \; (\_L \; S^q) \qquad \text{Eq. 3}$$

$$D_{peak} = \delta \; (S^r \_L/EI) \qquad \text{Eq. 4}$$

The quantities in parenthesis depend on arch size, arch configuration, support conditions, type and intensity of loading. Symbols for the various loading conditions, to be added to the equations 1 through 4, are given in Table III. The deflection equation (Eq. 4) is valid only for stress conditions within the elastic limit of the arch material. A negative value of D indicates a downward deflection of the arch peak.

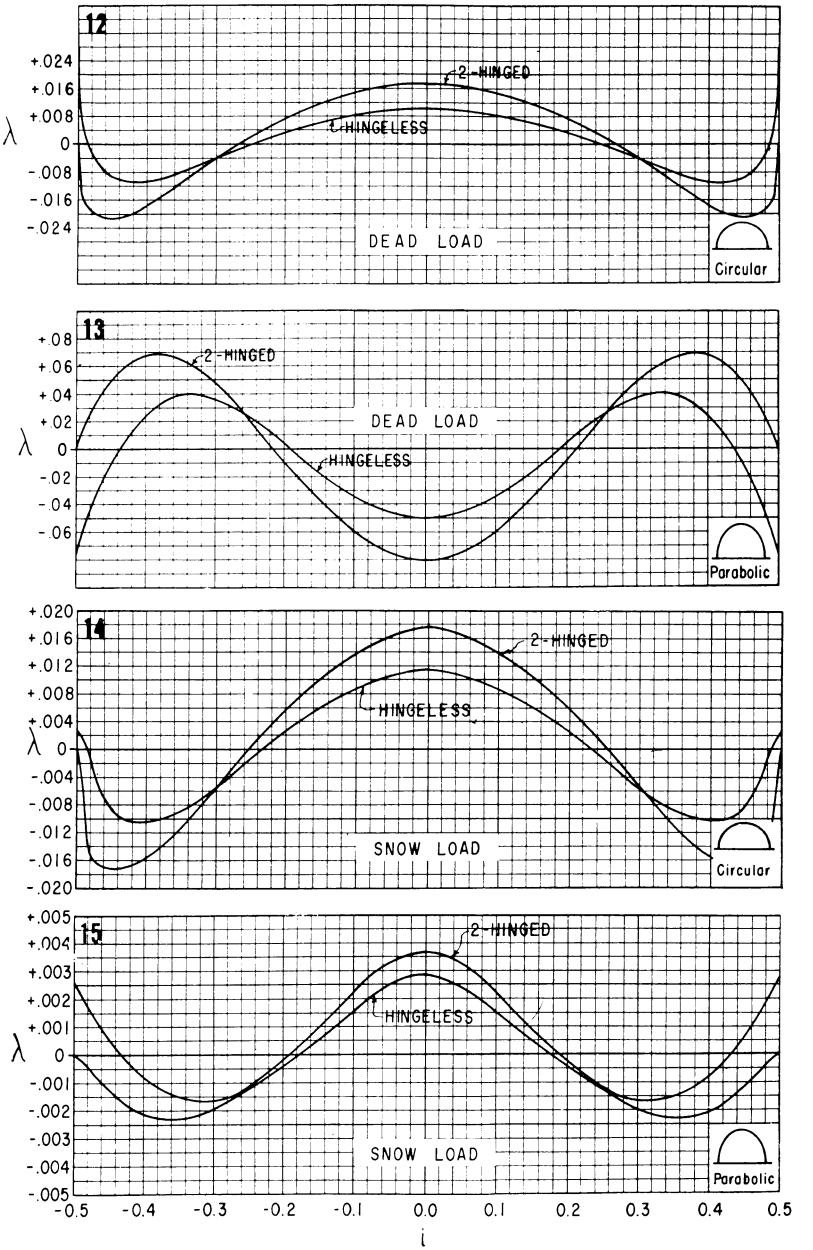

Figures 12, 13, 14 and 15. Dimensionless parameters for shell arch analysis.

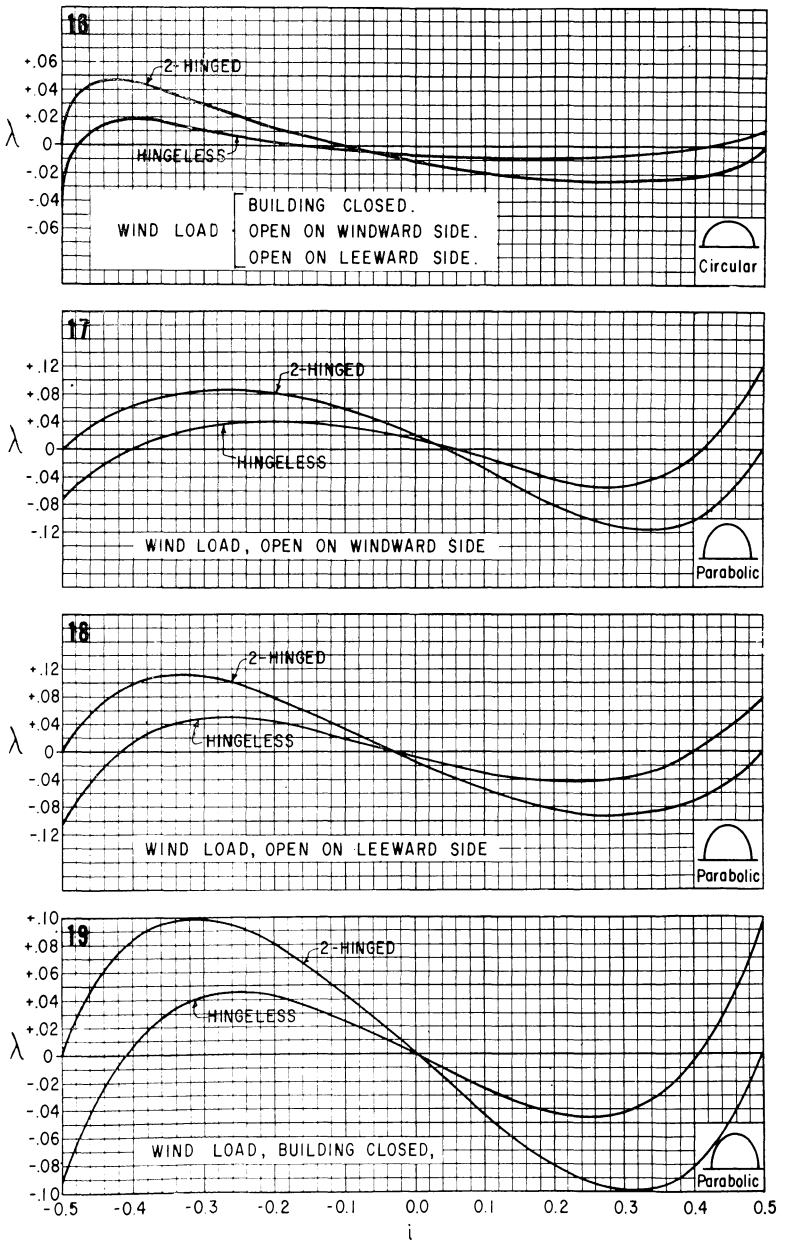

Figures 16, 17, 18 and 19. Dimensionless parameters for shell arch analysis.

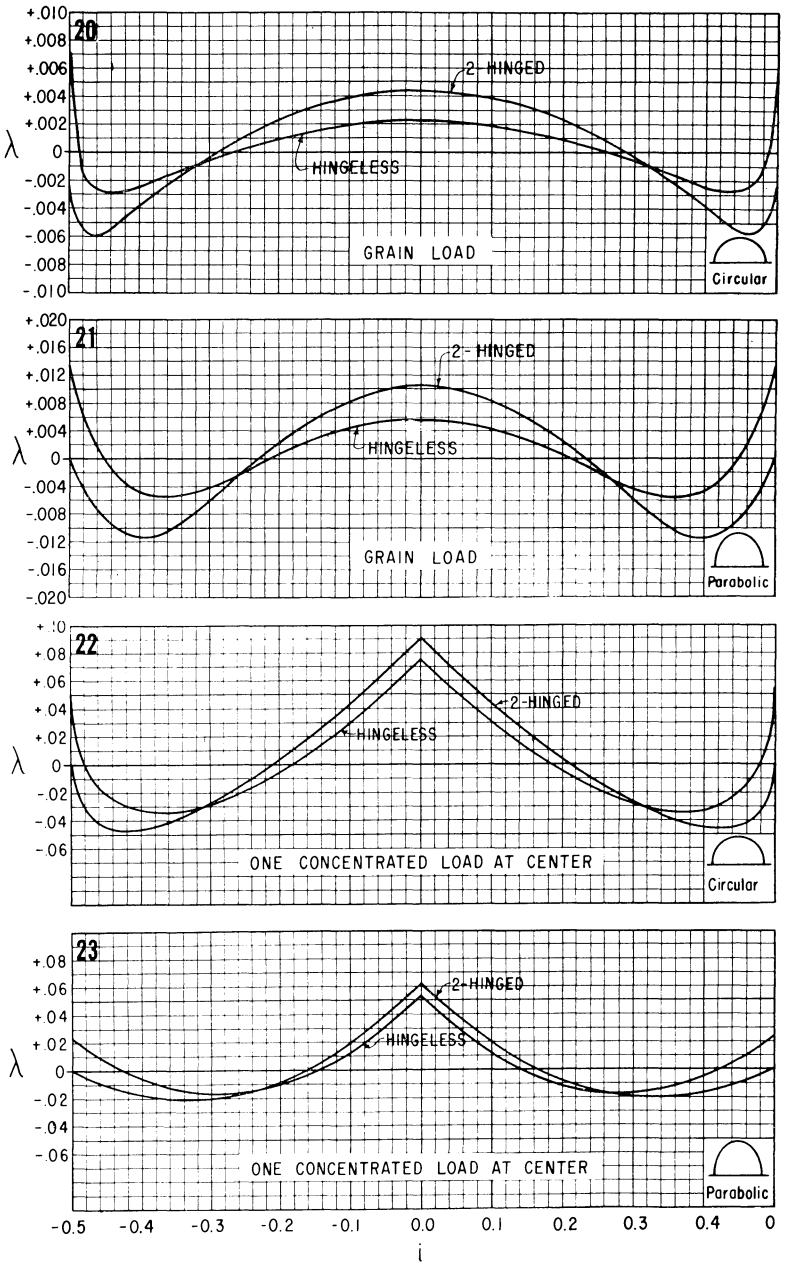

Figures 20, 21, 22 and 23. Dimensionless parameters for shell arch analysis.

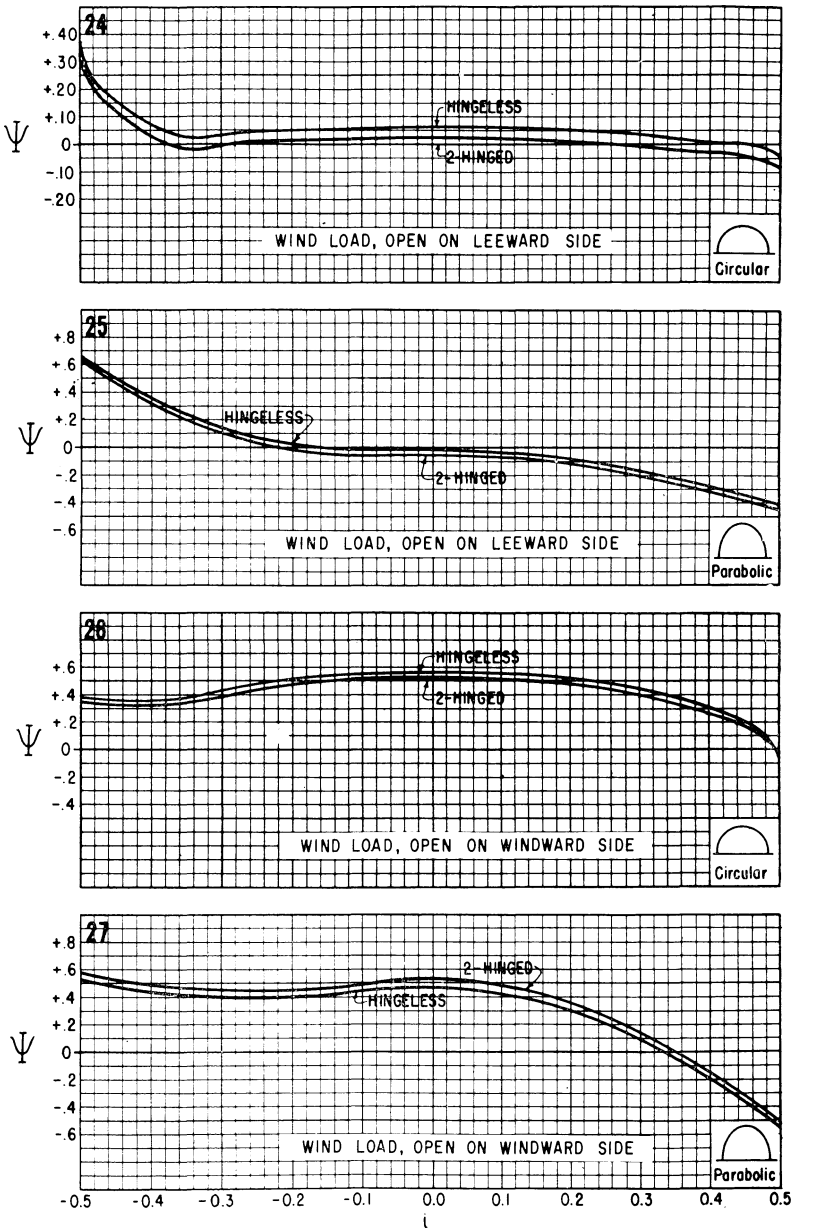

Figures 24, 25, 26 and 27. Dimensionless parameters for shell arch analysis.

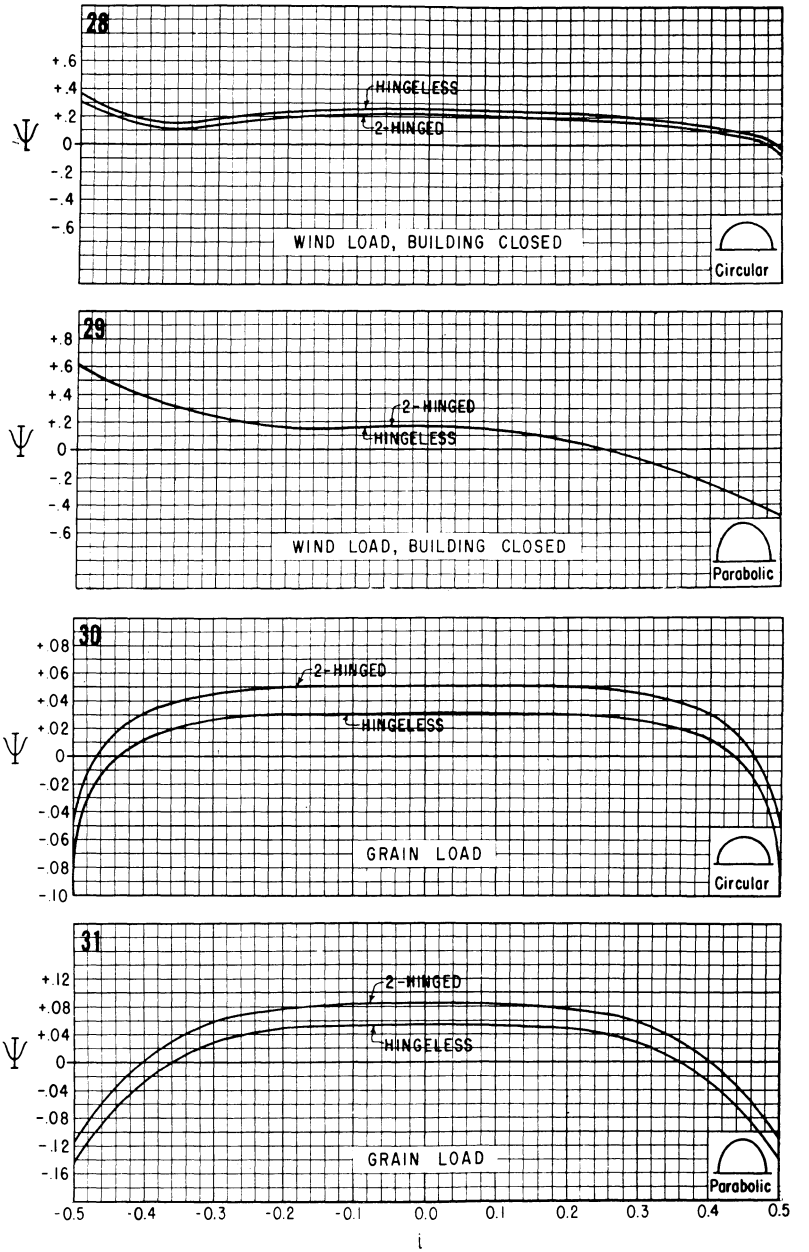

Figures 28, 29, 30 and 31. Dimensionless parameters for shell arch analysis.

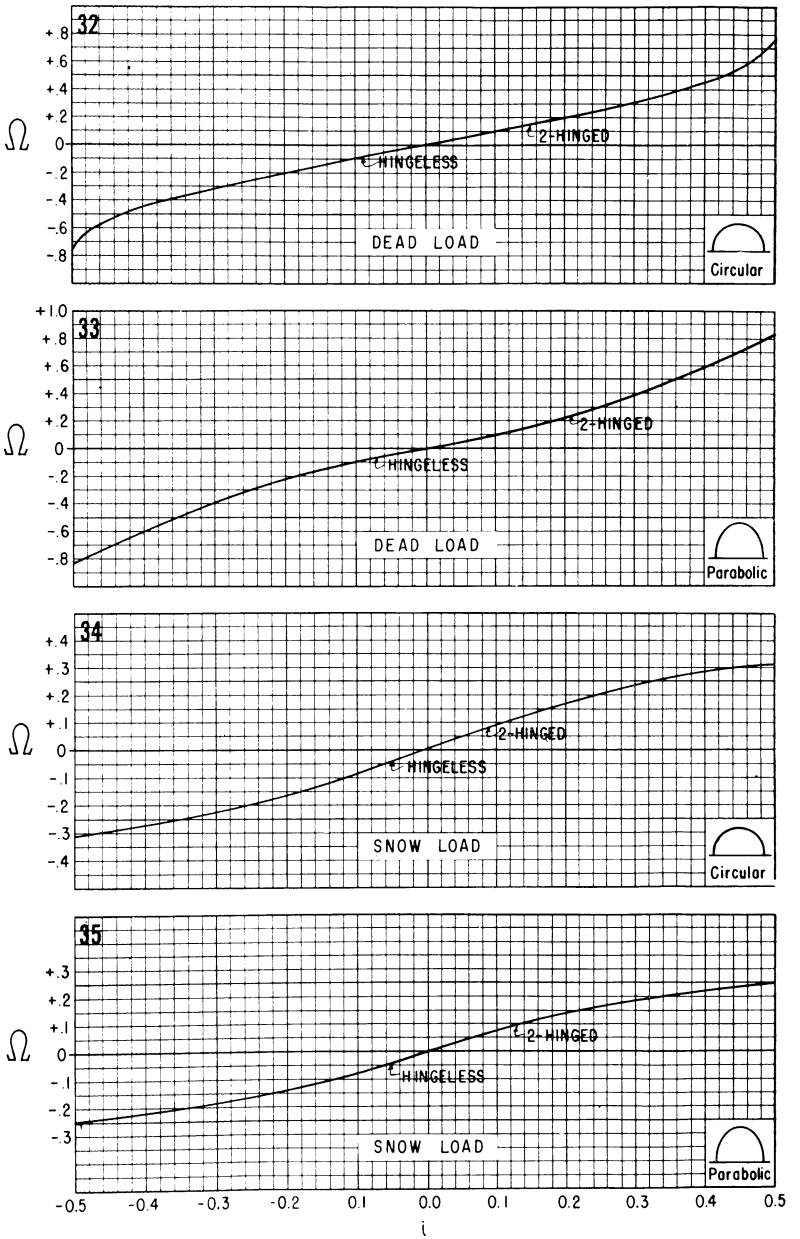

Figures 32, 33, 34 and 35. Dimensionless parameters for shell arch analysis.

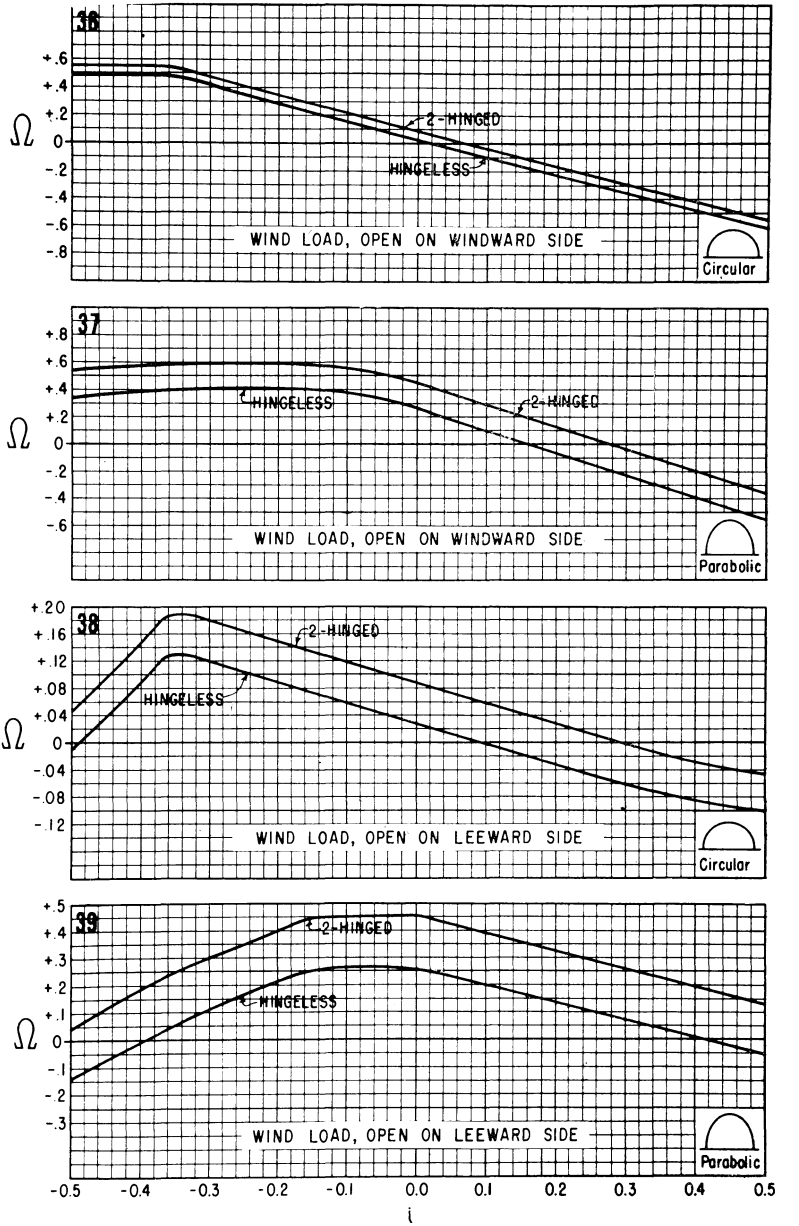

Figures 36, 37, 38 and 39. Dimensionless parameters for shell arch analysis.

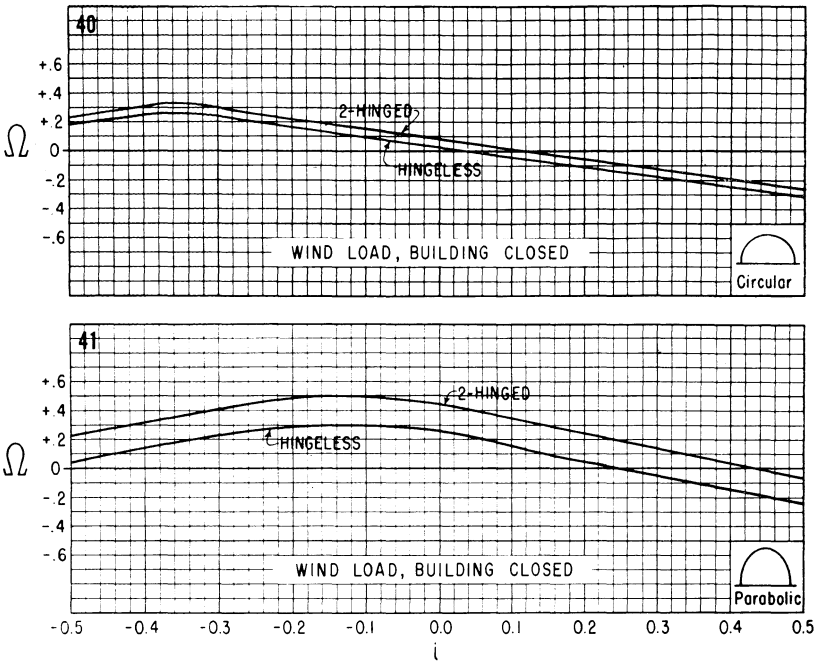

Figures 40 and 41. Dimensionless parameters for shell arch analysis.

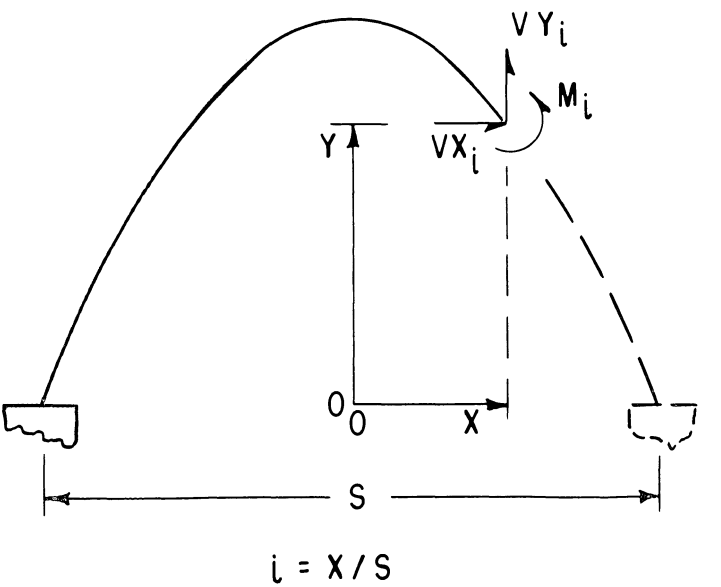

Figure 42. Sign convention for shears and moments.

Example of Analysis Using Dimensionless Parameters

It is desired to determine the location and value of the maximum moment and maximum shears in a circular arch structure with ideal hinged-end supports. Other conditions are:

Span, $S = 35$ feet
Dead load, DL $= 75$ lb/ft^2 (corresponding to an assumed roof thickness of 6 in.)
Wind load (Building closed) WL $= 20$ lb/ft^2 (equivalent wind speed of 87 mph)
Snow load, SL $= 25$ lb/ft^2 (Central States location)

Using design equations 1, 2, and 3 and entering the appropriate values, computation equations as shown in Table VI are obtained.

A computation sheet as shown in Table VII can be used to facilitate the final analysis of moments and shears. The number of points investigated in the arch depends upon the judgment of the analyst. Inspection of the moment parameter, λ graphs, Figures 12, 14, and 16 reveals rapid changes near the ends of the arch. Therefore, more points should be investigated in that area. Coefficients from the figures and tables as cross-referenced in Table III for each loading and stress are inserted in the computation equations listed in Table VI and the results entered on the computation sheet, Table VII. It was considered unlikely that both wind load and snow load would occur simultaneously. Therefore only the load which gave the *larger final result* was added to the dead load effect.

TABLE VI—Prediction Equations for Example of Arch Analysis.

Loading	Bending Moment	Horizontal Shear	Vertical Shear
	$M_i = \lambda_i\_L\ S^p$	$VX_i = \Psi_i\_L\ S^q$	$VY_i = \Omega_i\_L\ S^q$
Wind load	$= \lambda_i 20(35)^2$ $M_i = \lambda_i 24{,}500$ (Fig. 16)	$= \Psi_i 20(35)$ $VX_i = \Psi_i 700$ (Fig. 28)	$20(35)$ $VY_i = \Omega_i 700$ (Fig. 40)
Snow load	$= \lambda_i 25(35)^2$ $M_i = \lambda_i 30{,}625$ (Fig. 14)	$= \Psi_i 25(35)$ $VX_i = \Psi_i 875$ (Table IV)	$= \Omega_i 25(35)$ $VY_i = \Omega_i 875$ (Fig. 34)
Dead load	$= \lambda_i 75(35)^2$ $M_i = \lambda_i 91{,}875$ (Fig. 12)	$= \Psi_i 75(35)$ $VX_i = \Psi_i 2{,}625$ (Table IV)	$= \Omega_i 75(35)$ $VY_i = \Omega_i 2{,}625$ (Fig. 32)

TABLE VII—Stress Computations for Analysis of Two-Hinged Circular Shell Arch.

Stress Analyzed	Line No.	Computation Equations From Table VI	Load	Location Index, i: −0.50	−0.46	−0.42	−0.20	0	+0.20	+0.42	+0.46	+0.50
	1	$\lambda_i \times 24{,}500$	Wind, Bldg Closed	0	1030	1080	294	−270	−590	−490	−368	0
Bending	2	$\lambda_i \times 30{,}625$	Snow	0	−520	−510	184	545	184	−510	−520	0
Moment	3	$\lambda_i \times 91{,}875$	Dead	0	−1920	−1830	730	1560	730	−1830	−1920	0
	4	Select Stress	Max. Wind or Snow	0	−520	−510	294	545	294	−510	−520	0
	5	Line 3 + 4		0	−2440	−2340	1024	2105	1024	−2340	−2440	0
	6	Critical Bending Moment			−2440						−2440	
	7	$\Psi'_i \times 700$	Wind, Bldg Closed	210	147	110	140	147	140	55	30	−60
Horizontal	8	$\Psi'_i \times 875$	Snow	−134		(Constant throughout span)						
Shear	9	$\Psi'_i \times 2{,}625$	Dead	−662		(Constant throughout span)						
	10	Select Stress	Max. Wind or Snow	−134		(Constant throughout span)						
	11	Line 9 + 10		−796		(Constant throughout span)						
	12	Horizontal Shear at Critical Moment			−796						−796	
	13	$\Omega_i \times 700$	Wind, Bldg Closed	156	185	210	145	65	−35	−140	−160	−185
Vertical	14	$\Omega_i \times 875$	Snow	−270	−260	−245	−140	0	140	245	260	270
Shear	15	$\Omega_i \times 2{,}625$	Dead	−1920	−1520	−1260	−530	0	530	1260	1520	1920
	16	Select Stress	Max. Wind or Snow	−270	−260	−245	−140	0	140	245	260	270
	17	Line 15 + 16		−2190	−1780	−1505	−670	0	670	1505	1780	2190
	18	Vertical Shear at Critical Moment			−1780						1780	

Notes: (a) Units for Stresses Tabulated are:
Bending Moment — ft-lb/1 ft. wide arch section.
Shear — lb/1 ft. wide arch section.
(b) Algebraic sign is plus, unless minus (−) sign is shown.

Figure 43 shows a graphic solution for radial shear and direct stress at "i" equal 0.46; and at the arch support, where "i" is 0.50. The value of radial shear, VR, is necessary in designing the section. The direct stress, VT, must be taken into account together with bending stresses to determine the resultant tensile and compressive stresses.

The arch should be designed to resist the stresses at the point of critical bending moment, Figure 44. Then, it should be investigated for the combination of shear and direct stress in Figure 45.

Comparison of Arch Shape and End Conditions for Various Loads

An analytical comparison was made between circular and parabolic arches with fixed and hinged ends for each of the loadings considered. This comparison for maximum moments is shown in Figure 46. For vertical loadings, the parabolic arch has smaller moments; but for horizontal loadings the circular arch moments are smaller. Figure 46 should not be interpreted to mean that the maximum moments for the various

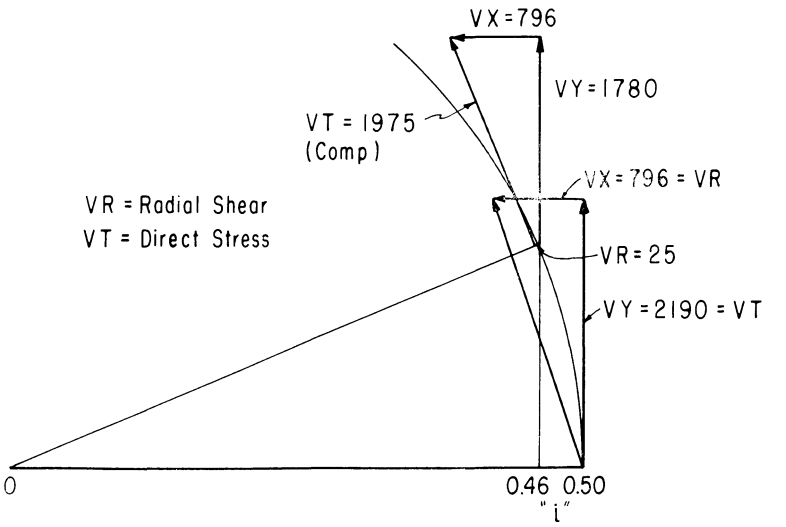

Figure 43. Graphical solution for radial shear and direct stress.

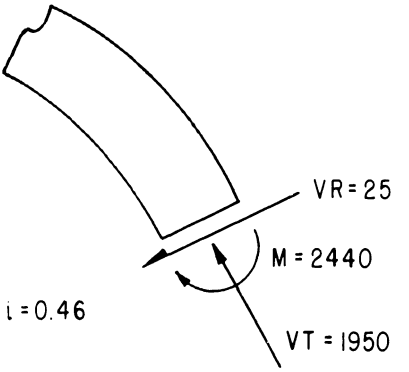

Figure 44. Stresses at point of maximum moment, example of arch shell analysis.

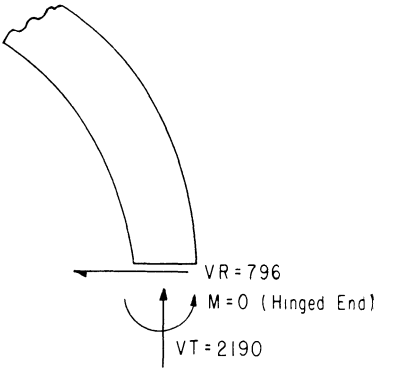

Figure 45. Stresses at point of maximum shear, example of arch shell analysis.

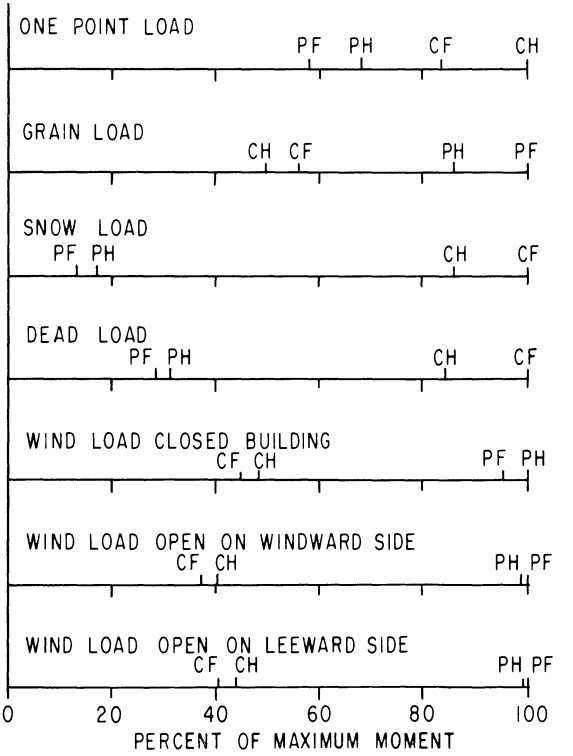

Figure 46. Comparison of moments in concrete arch shell analysis.

loadings are the same; but rather the moments vary according to equation 1. Thus, for changes in arch span, moments for some loads vary directly with span while for other loads, moments increase as a function of the second or third power of span.

Conclusions

Through the use of similitude, and dimensional analysis, dimensionless parameters can be written and evaluated to predict moments and shears in all statically indeterminate arches of similar outline configuration and having the same type of loading and end conditions.

Theoretical stiffness, gained by fixed end arches compared with hinged end arches, averaged about 100 percent.

Stiffness of fixed and hinged end arches measured with model arches by laboratory load-testing did not differ appreciably. This result was attributed to the inability to produce ideal fixed or hinged end support conditions in the laboratory.

The difference in ultimate load for fixed end compared to hinged end arches was not significant when three equal point loads were applied. The actual failure loads of the fixed end arches were 44 percent greater than predicted by the elastic theory. Failure loads for hinged end arches were 25 percent greater.

Repeated loading of the arches did not significantly change arch response to loading.

Stiffness moduli determined experimentally by deflection measurements ranged approximately from 1.5 to 15 times that predicted by conventional reinforced concrete design assumptions.

Circular arches are subjected to larger moments for vertical loadings while parabolic arches have larger moments under horizontal loads.

In design work, it is advisable to investigate a given arch for both fixed and hinged end conditions since ideal fixed or hinged ends are not likely to be achieved in actual construction.

Literature Cited

1. Barre, H. J. and L. L. Sammet. *Farm Structures.* New York: John Wiley & Sons, Inc., 1950.

2. Bureau of Yards and Docks. *Basic Structural Engineering.* Technical Publication NAVDOCKS TP -TE-3. Washington: Department of the Navy, 15 May 1954.

3. Housing and Home Finance Agency. *Snow Load Studies.* Housing Research Paper No. 19. Washington: Government Printing Office, May, 1952.

4. Mensch, Robert L., Theoretical and experimental investigation of concrete shell arches for utility buildings. Unpublished M.S. Thesis. Library, Oklahoma State University, 1962.

Oklahoma's Wealth in Agriculture

Agriculture is Oklahoma's number one industry. It has more capital invested and employs more people than any other industry in the state. Farms and ranches alone represent a capital investment of four billion dollars—three billion in land and buildings, one-half billion in machinery and one-half billion in livestock.

Farm income currently amounts to more than $700,000,000 annually. The value added by manufacture of farm products adds another $130,000,000 annually.

Some 175,000 Oklahoman's manage and operate its nearly 100,000 farms and ranches. Another 14,000 workers are required to keep farmers supplied with production items. Approximately 300,000 full-time employees are engaged by the firms that market and process Oklahoma farm products.

2-64/2½M